Identifiability of Helicopter Models Incorporating Higher-Order Dynamics

Stewart S. Houston*
Royal Aerospace Establishment, Bedford, MK41 6AE, England, United Kingdom
and
Colin G. Black†
University of Glasgow, Glasgow, G12 8QQ, Scotland, United Kingdom

This paper examines the identification of a linearized mathematical model of a Puma helicopter from experimental data gathered during flight tests in hover. The objective has been to study the sensitivities of the model parameters to the choice of approach available. The model of the helicopter represents the vertical response of the aircraft to collective pitch, but has been extended to incorporate higher-order rotor dynamics associated with blade flapping and induced velocity degrees of freedom. The approaches used in the identification of the model are frequency-domain based: output error and transfer function matching of frequency responses identified using time series methods. Examples of the identification of helicopter models incorporating higher-order rotor dynamics using rotor measurements from flight data are new. It is concluded that models of helicopter behavior that include higher-order dynamics can be identified successfully from flight data, but engineering judgment is the key to successful application of the methods and interpretation of the results.

Nomenclature

A = system matrix
a = blade lift-curve slope, 1/rad
B = control matrix
C_l' = lift deficiency factor
C_t' = thrust deficiency factor
g = acceleration due to gravity, m/s^2
I_β = blade flap inertia, kgm^2
k = empirical momentum correction factor
k_b = factor on blade first moment of mass
M_β = blade first moment of mass, kgm
m = helicopter mass, kg
m_a = additional air mass, kg
N = number of blades
R = rotor radius, m
T = rotor thrust, N; transpose when used as superscript
u = control vector
v_i = induced velocity, m/s—positive down
$\bar{v}_i$ = induced velocity normalized by rotor tip speed, $= v_i/\Omega R$
w = helicopter vertical velocity, m/s—positive down
x = state vector
β_0 = rotor coning angle, rad
γ = rotor Lock number, $\rho acR^4/I_\beta$
θ_0 = collective pitch angle, rad
ν_β = flap frequency ratio
ρ = air density, kg/m^3
σ = rotor solidity, total blade area/rotor disk area
Ω = rotorspeed, rad/s

Stability and Control Derivatives

f_{v_i}, i_{v_i}, Z_{v_i} = coning, induced velocity, and vertical acceleration derivatives with respect to (w.r.t.) induced velocity
$f_{\dot{\beta}_0}$, $i_{\dot{\beta}_0}$, $Z_{\dot{\beta}_0}$ = coning, induced velocity, and vertical acceleration derivatives w.r.t. coning velocity
f_{β_0}, Z_{β_0} = coning and vertical acceleration derivatives w.r.t. coning angle
f_w, i_w, Z_w = coning, induced velocity, and vertical acceleration derivatives w.r.t. vertical velocity
f_{θ_0}, i_{θ_0}, Z_{θ_0} = coning, induced velocity, and vertical acceleration derivatives w.r.t collective pitch

Introduction

MATHEMATICAL modeling of helicopters for handling qualities, performance, and flight control has always been a challenging area, and is one that continues to demand increasing attention from the community. This is because deficiencies in fidelity are widespread, affecting the validity of piloted simulation and control law design, hence potentially increasing the cost of developing new aircraft. System identification is proving to be a powerful tool for assisting in the validation of rotorcraft mathematical models, including those that incorporate higher order dynamics associated with rotor flapping and air mass behavior. Recent work[1-9] has made significant contributions in this new area, but has highlighted potential difficulties associated with the identifiability of such models, which could conceivably limit the usefulness of system identification as a model validation tool. These concerns center around incomplete measurement sets, the need to constrain variables, and choice of identification method as well as variable sensitivity to choice of test run and frequency range for modeling. This paper seeks to address these issues by example.

Background

The identification of helicopter mathematical models that incorporate higher order dynamics is relatively new; references have appeared mostly over the last few years.[1-9] Most of this work has focused on obtaining an acceptable model of helicopter vertical response to collective in hover,[1-6] although there has been some examination of forward flight cases in the midspeed range.[7-9] There has been some success in identifying

Received Oct. 3, 1989; revision received June 26, 1990; accepted for publication June 26, 1990.

*Senior Scientific Officer, Flight Dynamics Division; currently at University of Glasgow, Glasgow, G128 QQ, Scotland, United Kingdom.

†Research Assistant, Department of Aerospace Engineering.

higher-order dynamics, to the extent that results have been used to support the development of a generic helicopter simulation model.[10] The theme common to all this work, however, has been a concern over the identifiability and sensitivity of the model parameters. This sensitivity can be assessed as the degree to which the model parameters exhibit variation with method, data set, frequency range, etc. These variations arise, of course, because of the uncertainty associated with experimental data and model structure, but are widened by freedom to use engineering judgment at every stage in the identification process.

Theoretical Modeling

The response of the helicopter to collective pitch inputs in hovering flight can be described by a model incorporating those higher order dynamics of concern in this paper. The model incorporates first-order inflow and vertical velocity response, together with second-order coning. The model structure is written in constant coefficient, state-space form as

$$\dot{x} = Ax + Bu \tag{1}$$

where

$$A = \begin{bmatrix} i_{v_i} & 0 & i_{\dot{\beta}_0} & i_w \\ 0 & 0 & 1 & 0 \\ f_{v_i} & f_{\beta_0} & f_{\dot{\beta}_0} & f_w \\ Z_{v_i} & Z_{\beta_0} & Z_{\dot{\beta}_0} & X_w \end{bmatrix}, \quad B = \begin{bmatrix} i_{\theta_0} \\ 0 \\ f_{\theta_0} \\ Z_{\theta_0} \end{bmatrix} \tag{2}$$

$$x = [v_i \quad \beta_0 \quad \dot{\beta}_0 \quad w]^T, \qquad u = \theta_0 \tag{3}$$

Chen and Hindson[11] provide analytical expressions for these stability and control derivatives, which exhibit the following relationships

$$Z_{v_i} = -Z_w, \quad f_{v_i} = -f_w, \quad i_w = -1.5Ri_{\beta_0}$$

$$f_{\theta_0} = -\Omega f_{\dot{\beta}_0}, \quad Z_{\theta_0} = -\Omega Z_{\dot{\beta}_0} \tag{4}$$

This model assumes constant rotor speed, the derivatives do not take hinge offset into account, fuselage aerodynamics and the interference between rotor and fuselage flowfields is neglected, the blades are assumed to be rigid, and unsteady effects are not represented. This model formed the basis for some earlier work in this area,[1-4] which suggested that substantial improvements in the correlation between flight and theory could be obtained if some additional effects were included. These were the following: 1) empirical correction of the momentum-derived uniform component of inflow, to account for the real nonuniformity, tip loss, and root cutout effects; 2) inclusion of lift deficiency factors to account for unsteady effects in the real wake; and 3) reduction of blade first moment of mass, so that the rigid blade model made some approximation to the hub inertia force reactions experienced with real, flexible blades.

For this paper, the stability and control derivatives in the A and B matrices were obtained by a numerical forward and backward differencing of the full nonlinear equations (incorporating these additional features), which are as follows. The momentum expression for thrust is

$$T = m_a\bar{v}_i + 2\rho(3.142R^2)C_t'v_i/k(v_i/k - w + \tfrac{2}{3}R\dot{\beta}_0) \tag{5}$$

From Johnson,[12] C_t' is

$$C_t' = \frac{1}{1 + a\sigma/(16\bar{v}_i)} \tag{6}$$

The blade element expression for rotor thrust, to balance that given by Eq. (5), is

$$T = \tfrac{1}{4}\Omega R\rho a\sigma(3.142R^2)(\tfrac{2}{3}\Omega R\theta_0 - v_i + w - \tfrac{2}{3}R\dot{\beta}_0) \tag{7}$$

Again from Johnson,[12] the equation for blade flapping is

$$I_\beta\ddot{\beta}_0 + \gamma\Omega I_\beta/8C_1'\dot{\beta}_0 - k_bM_\beta\dot{w} = -I_\beta\gamma\Omega C_1'/(6R)v_i - I_\beta\Omega^2\nu_\beta^2\beta_0 + I_\beta\gamma\Omega C_1'/(6R)w + I_\beta\Omega^2\gamma C_1'/8\theta_0 \tag{8}$$

The hub force equation is

$$NI_\beta\Omega\gamma/(6mR)\dot{\beta}_0 + Nk_bM_\beta/m\ddot{\beta}_0 - \dot{w} = -NI_\beta\gamma\Omega/(4mR^2)v_i + NI_\beta\gamma\Omega/(4mR^2)w + NI_\beta\gamma\Omega^2/(6mR)\theta_0 - g \tag{9}$$

C_1' is the lower harmonic loading limit of Loewy's lift deficiency function, given by

$$C_1' = \frac{1}{1 + 3.142\sigma/(4\bar{v}_i)} \tag{10}$$

With $k = k_b = C_1' = C_t' = \nu_\beta^2 = 1.0$, this model in linearized form is identical to that given in Ref. 11. When configured as a Puma, trimmed in the hover, and linearized with $k = 1.4$ and $k_b = 0.7$ (values suggested in Ref. 4), the thrust and lift deficiency terms are $C_t' = 0.72$, $C_1' = 0.55$, and the A and B matrices corresponding to Eqs. (2) are

$$A = \begin{bmatrix} -9.197 & 0 & -36.54 & 7.311 \\ 0 & 0 & 1 & 0 \\ -2.294 & -821.9 & -18.75 & 3.317 \\ 0.755 & -102.3 & 2.868 & -0.628 \end{bmatrix}, \quad B = \begin{bmatrix} 589.0 \\ 0 \\ 517.5 \\ -79.14 \end{bmatrix} \tag{11}$$

Note immediately that two of the relational constraints shown in Eqs. (4), specifically $f_{v_i} = -f_w$ and $Z = -Z_w$, are no longer valid. This is because C_1' is a function of v_i. Equation (12) shows the equations of motion when Chen and Hindson's original model is configured as a Puma. Note that the modeling enhancements outlined earlier substantially modify the values of most of the derivatives. In particular, note that all except one of the Z-force derivatives have opposite signs

$$A = \begin{bmatrix} -11.44 & 0 & -39.27 & 7.856 \\ 0 & 0 & 1 & 0 \\ -5.692 & -848.6 & -32.16 & 5.692 \\ -0.168 & -177.8 & -1.618 & 0.168 \end{bmatrix}, \quad B = \begin{bmatrix} 589.4 \\ 0 \\ 887.7 \\ 44.66 \end{bmatrix} \tag{12}$$

Flight Test Data Base and Identification Methods

The test data base available contained pilot-generated frequency sweeps of the collective lever, conducted in a free-air hover. These were used for identification. Additionally, collective step inputs were used to provide a dissimilar input type for use in verifying the models identified from the sweeps. Seven separate frequency sweep runs were available for analysis. The multiblade collective pitch and coning were derived from the individual measurements available from each blade. Except where indicated in the paper, one of the seven sweep data sets available was used to illustrate the point under discussion. The data set used is shown in Fig. 1, which illustrates the pilot collective lever sweep, the multiblade coning and collective angles, and the vertical acceleration. Blade lag, rotor speed, and torque measurements were available, but visual inspection justified the omission of these additional degrees of freedom. Not only were lag and rotorspeed perturbations very small for control input amplitudes shown in Fig. 1, but lag variations were attenuated at frequencies above 0.4 Hz and rotor speed variations above about 0.8 Hz. These response bandwidths are in contrast to those of the variables shown here, which extend up to 4 Hz. It should be noted that omission of these additional degrees of freedom may not in gen-

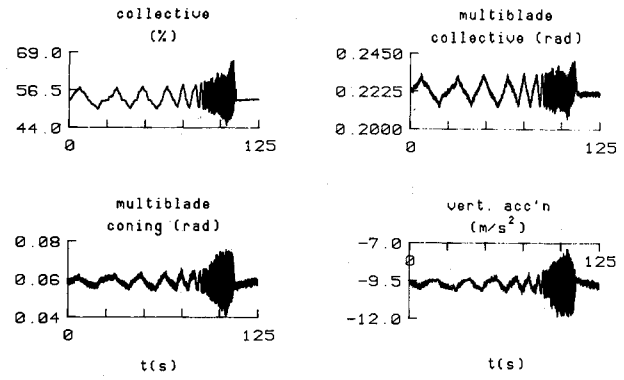

Fig. 1 Collective lever frequency sweep and resulting aircraft response: Puma XW241; mass 5250 kg; hover 3000 ft.

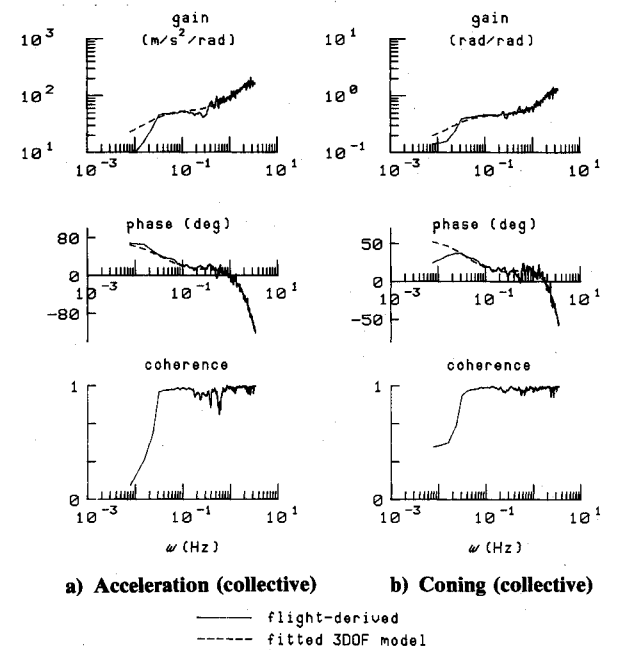

Fig. 2 Frequency responses derived from collective sweep input, with best least-squares match given by 3-DOF model structure.

eral, be appropriate if an acceptable model of vertical response dynamics in hover is to be achieved.[5,6]

The two identification methods used in this paper were frequency-domain based. The first method uses an output-error approach, where the outputs are based on the coning and vertical acceleration information. The state-space model is represented in terms of Fourier-transformed quantities and an appropriate output-error identification carried out to determine the matrix coefficients. Details of this approach, in general, can be found in Ref. 13, and mathematical details relating to this particular application can be found in Ref. 14. The second method involved using time series analysis techniques to derive frequency responses representing transfer functions for the system, which were used with a model-matching process to find model parameters that allow the model structure to fit, in a least-squares sense, the derived frequency responses. References 15 and 16 are standard texts that deal with the theory of time series analysis methods; Ref. 17 describes the method of transfer function matching used here. Its application to this problem is detailed elsewhere.[2]

Results

Comparison of Transfer Function Matching and Output-Error Methods

With regard to the transfer function fitting approach, Fig. 2 shows the flight-derived coning and vertical acceleration to collective frequency responses, together with the corresponding input-output coherences. Also shown is the best fit of these data in a least-squares sense to the model structure given by Eqs. (2). Any point with coherence <0.8 is not, however, used in the fitting process. All 14 derivatives were identified without constraint and are given in Table 1. Note that both coherence plots are very close to unity across most of the frequency range, falling below 0.8 only at the first few frequency points, a region where the pilot's input has low content. Note also that the fit offered by the coupled three degree-of-freedom (DOF) model structure is excellent, again across the frequency range, with the exception of a few points at the very low frequency end of the response.

Figure 3 shows corresponding results, to those illustrated in Fig. 2, from the output-error approach, giving similarly good fits, in this case, to the extent that it is difficult to discern predicted from flight-derived values (phase comparisons have not been shown). It should be noted that some convergence difficulties were encountered with the output-error method when attempts were made to estimate all 14 parameters independently, and it was found necessary to fix the derivatives in the dynamic inflow equation. No measurements were available for the induced velocity v_i present as a state in the model. Alternative approaches include the use of a rank-deficient information matrix[18] or the incorporation of defined relationships into the model. Since the identified derivative values varied with the constraints used, the values identified by transfer function matching were used to fix the dynamic inflow equation derivatives in the output-error method in order to lend consistency to the comparison between the two approaches. It can be seen that there is fairly good agreement between theory and experiment, and with only a few exceptions, both identification methods give very similar derivative values. It would appear that the preferred approach to use is that of transfer function matching since no constraints need to be applied for a viable solution to be obtained, unlike the output-error approach. However, with the use of appropriate constraints, the output-error approach may be equally preferred. The question of the use of constraints, with output-error and transfer function approaches, is addressed in the final part of the Results section of this paper.

Parameter Sensitivity to Test Run

For illustrative purposes, the identification results presented so far have focused on only one of the seven sets of test data available. However, the other six sets do allow corresponding models to be identified, which in turn allows an assessment of the impact of any random run-to-run effects on the derivative values. This in turn gives an indication of how confident one might be in the results from any given single run. Should scatter be apparent, then the derivatives can be combined by

Table 1 Comparison of derivatives identified by frequency response and output-error methods

Derivative	Theoretical value	Frequency response[a]	Output error[a]
i_{v_i}	−9.197	−9.147 (0.0472)	−9.147[b] ——
i_{β_0}	−36.54	−40.76 (0.5602)	−40.76[b] ——
i_w	7.311	6.703 (0.0892)	6.703[b] ——
i_{θ_0}	589.0	599.4 (3.0945)	599.4[b] ——
f_{v_i}	−2.294	−4.245 (0.0248)	−4.706 (0.28)
f_{β_0}	−821.9	−836.7 (1.5973)	−857.1 (8.55)
$f_{\dot{\beta}_0}$	−18.75	−24.47 (0.0855)	−25.15 (0.48)
f_w	3.317	4.635 (0.0443)	3.701 (0.88)
f_{θ_0}	517.5	682.8 (1.3974)	699.8 (12.7)
Z_{v_i}	0.755	0.547 (0.0056)	0.291 (0.07)
Z_{β_0}	−102.3	−96.46 (0.4640)	−101.1 (8.09)
$Z_{\dot{\beta}_0}$	2.868	1.393 (0.0164)	4.833 (0.61)
Z_w	−0.628	−0.474 (0.0315)	−0.532 (0.11)
Z_{θ_0}	−79.14	−48.87 (0.3510)	−35.26 (6.95)

[a]Parameter standard deviation in parentheses.
[b]Values fixed at frequency response method values.

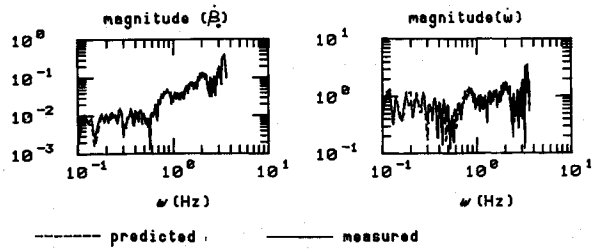

Fig. 3 Comparison of measured and predicted magnitudes of the Fourier-transformed measurements.

an averaging process into a single model to try and accommodate in a statistical way the effects that have led to the variation in the derivative values. Run-to-run differences amongst the derivatives could be due to various things, but those of concern here are due to differences in rotor operating state and flight condition or holes in the spectra of the particular sweep input that lead to frequency regions of poor coherence. In the approach used to generate the results for this paper, the frequency response fitting process can discard such points, and it is this identification approach that was used to generate the results for this section.

The seven individual values for each derivative, available from each of the seven identified models, were treated as a sample set of data for which average, spread, and sample standard deviation (SSD) were calculated. These results are shown in Table 2 together with results from the three best runs, which are discussed later. Spread and SSD are expressed as a percentage of the average value. Perhaps the spread is hardly surprising, given that the sum of the squares of the mismatch between the fitted model's frequency response and that identified from flight was, for the poorest fit, almost three times that of the best fit. No attempt has been made to explore correlation between the estimates, which could help to explain the spread.

In the case of each individual identified model, the variances associated with the derivative values were small, with the exception of that for i_{θ_0}. The frequency responses, however, had differences of detail, although each had the same form. These were usually associated with regions of poor coherence, which was itself a feature of the run-to-run comparisons. The spread in Table 2 has to be viewed first of all in this context of differing run-to-run coherence before any other contributions to the variability of derivatives with run used are considered. An additional point to note is that, in general, the parameter standard deviations do not reflect the actual spread among the seven identified models. This is consistent with other parameter estimation experiences; the reader is referred to the work of Maine and Iliff.[19]

Turning now to the results from the three best runs in Table 2, analysis of all seven vertical acceleration to collective results, in particular, revealed in-four of the seven cases that 15–25% of the points in the frequency response had coherence values <0.8, i.e., played no part in the fitting process and the determination of the derivative values. By contrast, $<5\%$ of the points in the other three had coherence values <0.8. Accordingly, average, spread, and SSD were recalculated using only these latter three cases, which are annotated as the results from the three best runs in Table 2. Note that both the spread and SSD are considerably reduced in comparison with those from all seven runs together. The spread of only one derivative out of these three models exceeds 30% of the average value, most being within 20%. Likewise, only one SSD value exceeds 30% of the average, most being within 15%. Note, however, that both sets of average values are generally similar. A tentative conclusion from this analysis is that robust model parameters can be derived from data with $<5\%$ of the coherence values below 0.8. Conversely, if $>15\%$ of the coherence points lie below 0.8, then the estimates are likely to exhibit wide spread in values. The results in Table 2 show that there is a slightly better correlation between theory and flight for results averaged from the best three runs than there is from all seven taken together, but for model validation, the true benefit of the former results is that the spread in the identified values is much less. This gives increased confidence in the use of these averaged values for the comparison with theory.

Parameter Sensitivity to A Priori Estimates

In this section, a specific case is used to illustrate how different a priori estimates (that is, the starting guess used for the iterative parameter searches) of some derivatives can influence the identified values and the resulting validation of the theoretical model. The transfer function matching approach is used, and the particular case involves the terms in the dynamic inflow equation

$$\dot{v}_i = i_{v_i} v_i + i_{\dot{\beta}_0} \dot{\beta}_0 + i_w w + i_{\theta_0} \theta_0 \tag{13}$$

which will take substantially different values depending on the value of the additional air mass m_a that is used. Throughout this paper, the value of air mass m_a used is that due to Carpenter and Fridovitch[20]; Eq. (14) shows the values of the dynamic inflow equation derivatives thus derived. The work of Pitt and Peters[21] gives a lower air mass value and the corresponding values are shown in Eq. (15)

$$\dot{v}_i = -9.197\, v_i - 36.54\, \dot{\beta}_0 + 7.311\, w + 589.0\, \theta_0 \tag{14}$$

Table 2 Summary of derivatives identified from seven test runs

Derivative	Theoretical value	Identified[a,b] value	Spread, %	Sample standard derivation, %	Identified[a,c] value	Spread, %	Sample standard derivation, %
i_{v_i}	−9.197	−8.842 (0.0571)	−21.6; +17.8	14.2	−8.797 (0.0387)	−2.1; +4.0	3.4
i_{β_0}	−36.54	−46.27 (0.7113)	−11.9; +29.8	14.7	−45.63 (0.5702)	−10.7; +5.7	9.2
i_w	7.311	6.941 (0.0900)	−7.1; +9.4	5.5	6.595 (0.0812)	−2.2; +0.6	2.0
i_{θ_0}	589.0	593.1 (3.7095)	−2.7; +2.8	2.1	593.9 (2.7173)	−0.7; +0.9	0.8
f_{v_i}	−2.294	−4.015 (0.0247)	−31.0; +45.9	27.0	−3.963 (0.0200)	−6.8; +7.1	6.2
f_{β_0}	−821.9	−819.8 (2.7015)	−5.4; +7.2	4.5	−813.1 (1.4626)	−1.8; +2.9	2.6
$f_{\dot{\beta}_0}$	−18.75	−23.48 (0.1385)	−23.9; +30.2	17.7	−23.42 (0.0725)	−2.3; +4.5	3.9
f_w	3.317	4.301 (0.0426)	−21.5; +34.7	19.7	4.307 (0.0380)	−9.1; +7.6	8.4
f_{θ_0}	517.5	645.8 (1.4591)	−15.1; +17.7	11.6	648.2 (1.2174)	−2.8; +5.3	4.6
Z_{v_i}	0.755	0.409 (0.0055)	−110.9; +56.1	53.6	0.553 (0.0018)	−14.5; +15.6	15.0
Z_{β_0}	−102.3	−110.2 (0.5260)	−38.1; +69.9	33.8	−86.47 (0.4097)	−21.1; +11.6	18.3
$Z_{\dot{\beta}_0}$	2.868	2.339 (0.0300)	−62.0; +83.6	59.5	1.780 (0.0168)	−21.7; +40.9	35.4
Z_w	−0.628	−0.402 (0.0099)	−95.5; +43.9	45.2	−0.402 (0.0084)	−7.9; +6.4	11.0
Z_{θ_0}	−79.14	−39.61 (0.3980)	−158.6; +76.0	73.7	−54.60 (0.0943)	−17.2; +27.7	24.2

[a]Averaged parameter standard deviation in parentheses.
[b]Averaged values from seven runs.
[c]Averaged values from best three data sets.

$$\dot{v}_i = -14.347\ v_i - 57.002\ \dot{\beta}_0 + 11.405\ w + 918.84\ \theta_0 \quad (15)$$

i.e., relative to Eq. (14), the derivatives are all increased by a factor of about 1.56. The derivatives identified using each set of a priori estimates are

$$\dot{v}_i = -8.797\ v_i - 45.631\ \dot{\beta}_0 + 6.595\ w + 593.896\ \theta_0 \quad (16)$$

$$\dot{v}_i = -9.229\ v_i - 51.653\ \dot{\beta}_0 + 9.643\ w + 911.012\ \theta_0 \quad (17)$$

where the former is that obtained with a priori values shown in Eq. (14), the latter using the values in Eq. (15). The results shown are based on the average of the three best data sets as defined in the previous section. The quality of fit of the transfer functions is the same in each case. This is an important result; it significant from the point of view of model validation. This is because, with the exception of the derivative i_{v_i}, the identified results are inconclusive regarding which value of m_a ought to be used in the theoretical model, the only compelling evidence to support the Carpenter and Fridovitch value, in both cases, being the term i_{v_i}. This sensitivity to a priori estimates is undoubtedly due to the fact that the identification is performed without the aid of any inflow information. It is emphasized that these results are not the result of a convergence problem with the algorithm used to fit the 3 DOF model structure to the flight-identified frequency responses. The corresponding transfer function polynomials are identical in each case. This indicates a problem in nonuniqueness of solution, the nature of the problem being that it is underdetermined, having only two frequency responses (and, hence, transfer functions) with which to determine a state-space model that is actually fully described by three transfer functions.

This result implies that, if the model is to be validated by comparison with identified derivatives, then the selection of the a priori estimates takes on some importance. The impact of this sensitivity issue on model validation can be assessed by examining the transfer function characteristics of the theoretical model, with both values of m_a. The value of m_a chosen for the theoretical model has a significant impact on the transfer function poles and zeros. Table 3 compares the poles of the theoretical model configured with both Carpenter and Fridovitch's[20] as well as Pitt and Peters'[21] value of m_a. In the case of the former, the inflow mode is considerably less well damped, although the coning mode is slightly better damped.

Table 4 compares the corresponding transfer function zeros. Perhaps the only important difference (since they lie in the right half, unstable part of the s plane) is in the complex pair in the vertical velocity to collective transfer function.

Table 3 Comparison of theoretical model transfer function poles

Mode	Carpenter-Fridovitch	Pitt-Peters
Inflow	−11.558	−18.417
Coning	$-8.411 \pm 25.344i$	$-7.565 \pm 24.908i$
Heave	−0.196	−0.202

Table 4 Comparison of theoretical model transfer function zeros

Transfer function	Carpenter-Fridovitch	Pitt-Peters
v_i/θ_0	(0.752), $(6.480 \pm 27.723i)$	(0.752), $(6.480 \pm 27.723i)$
β_0/θ_0	(0.094), (−6.800)	(0.095), (−10.506)
w/θ_0	(−4.991), $(0.608 \pm 39.016i)$	(−7.651), $(0.876 \pm 39.385i)$

Table 5 Comparison of solutions—three relational constraints vs no constraints

Derivative	Theoretical value	Unconstrained[a]	Three constraints[a]
i_{v_i}	−9.197	−9.147 (0.0472)	−9.271 (0.0500)
$i_{\dot{\beta}_0}$	−36.54	−40.76 (0.5602)	−35.79 (0.2709)
i_w	7.311	6.703 (0.0892)	7.161 —
i_{θ_0}	589.0	599.4 (3.0945)	578.2 (2.8634)
f_{v_i}	−2.294	−4.245 (0.0248)	−4.866 —
f_{β_0}	−821.9	−836.7 (1.5973)	−837.2 (0.3895)
$f_{\dot{\beta}_0}$	−18.75	−24.47 (0.0855)	−25.46 (0.1196)
f_w	3.317	4.635 (0.0443)	4.866 (0.0200)
f_{θ_0}	517.5	682.8 (1.3974)	705.2 (1.5643)
Z_{v_i}	0.755	0.547 (0.0050)	0.497 (0.0100)
Z_{β_0}	−102.3	−96.46 (0.4640)	−102.5 (0.4709)
$Z_{\dot{\beta}_0}$	2.868	1.393 (0.0164)	1.131 (0.0100)
Z_w	−0.628	−0.474 (0.0315)	−0.497 (0.0100)
Z_{θ_0}	−79.14	−48.87 (0.3510)	−43.28 (0.4254)

[a]Parameter standard deviation in parentheses.

Parameter Sensitivity to Frequency Range

Figure 4 shows how all 14 derivatives in the model vary with the frequency range used when identifying models using the transfer function matching approach. In all cases, the lowest frequency point forms the start of the frequency range, and each derivative is plotted against the upper limit in the frequency range. For convenience, the derivatives have all been normalized by the corresponding theoretical value given in Eq. (11). Normalized values of 1 indicate that theory and flight correlate identically—any value <0 would indicate that theory and flight derivatives had opposite sign. The agreement between theory and experiment is discussed later; in this section, the important feature examined is the point at which the derivative values cease to vary significantly with increasing frequency. With the coning and inflow derivatives, there is a definite trend with increasing frequency. In these cases, the identified derivatives cease to vary significantly with increasing frequency above about 3 Hz. Such a trend is not as

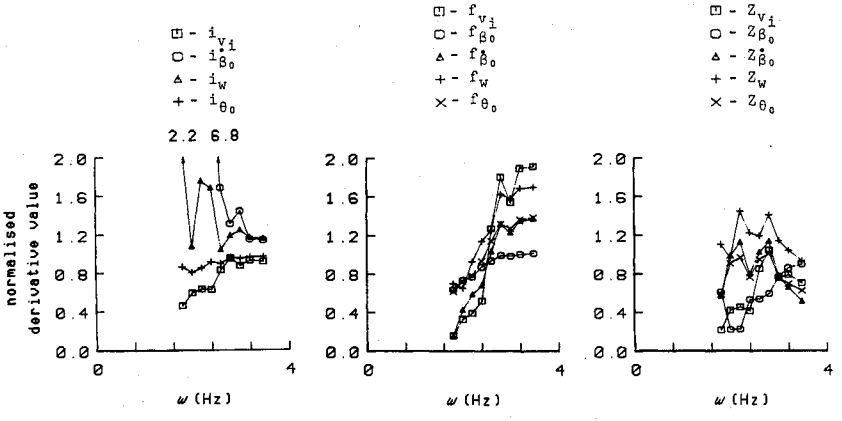

Fig. 4 Sensitivity of parameter estimates to frequency range—transfer function matching method.

obvious in the Z-force derivatives, and it is here that evidence suggests that the derivatives are still changing and, therefore, that even 3.5 Hz is an insufficient frequency range for robust identification of these derivatives. Perhaps such a result is not entirely surprising. It is the experience with these model-matching methods that resonant peaks, and just as important the following gain and phase rolloff, generally have to be included to define properly any model. In the particular case examined in this paper, the resonant peak in coning and vertical acceleration to collective is around 3-3.4 Hz, consistent with the result just observed. This tends to confirm then that one ought to identify across a frequency range appropriate to the bandwidth of the model. This is 3-4 Hz with this model because of the impact of the coning dynamics, which have a natural frequency just slightly in excess of 3 Hz.

Parameter Sensitivity to Constraints

Constraining parameters is a common feature of identification approaches. Sometimes it is done when limited information is available and the model has many parameters, and the method used may not converge onto a realistic solution, if at all. In such cases, a derivative may be fixed at a value that is theoretically based. Alternatively, the structure of the model to be validated may suggest some natural constraints that can be used to minimize the number of independent terms to be identified. Both types of constraints are explored in this section.

First, with reference to Eqs. (4), it can be seen that there are five relational constraints. Previous work,[2] however, showed that the constraints involving the control terms were not appropriate to invoke (this was attributed to unmodeled engine/rotor governing dynamics), leaving three. Solutions based on this approach were obtained using the transfer function matching method, and the results are shown in Table 5. Note that there are some differences, but, in general, both models are very similar. In the context of model validation, the differences shown in Table 5 are not significant.

Second, one of the derivatives was fixed at a theoretical value. A numerical constraint such as this is a common feature in identification, but is used here to illustrate that, across a broad frequency range, two very different solutions can have apparently very similar frequency responses. In addition, it is shown that the choice of one of the models over the other has a significant impact on model validation. The results presented can be found in the earlier work[2-4] and are included in this paper for completeness. The theoretical model derivatives are those given by Chen and Hindson's original model[11] configured as a Puma, i.e., Eq. (12). Further, the identified models were derived using a different test run to that used elsewhere in this paper. Finally, the three constraints $f_{v_i} = -f_w$, $Z_{v_i} = -Z_w$, and $i_{\beta_0} = -\frac{3}{2}Ri_w$ were active in the identification. The results are given in Table 6. One of the models has been identified with Z_{θ_0} constrained at the theoretical value. This is compared with the solution obtained with Z_{θ_0} free where it took the opposite sign. It is clear that theory, as given by Chen and Hindson's equations, i.e., without any of the additional modeling features outlined in this paper,

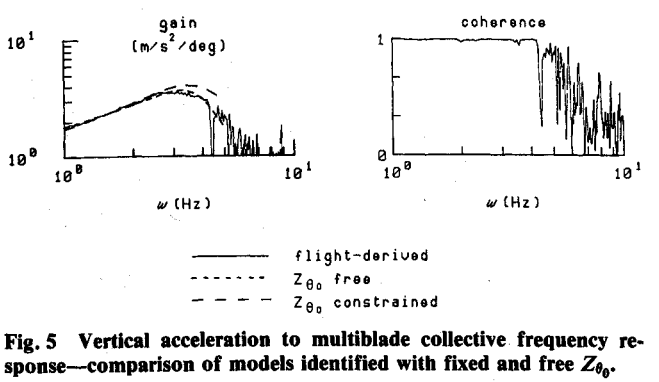

Fig. 5 Vertical acceleration to multiblade collective frequency response—comparison of models identified with fixed and free Z_{θ_0}.

Table 6 Use of numerical constraints—comparison of two identified models with theory

Derivative	Theoretical value	Identified[a]	Identified[b]
i_{v_i}	−11.441	−9.809	−8.553
i_{β_0}	−39.272	−41.955	−35.340
i_w	7.856	8.393	7.070
i_{θ_0}	589.4	606.3	578.8
f_{v_i}	−5.692	−5.650	−4.107
f_{β_0}	−848.6	−886.9	−803.7
$f_{\dot{\beta}_0}$	−32.16	−31.22	−22.52
f_w	5.692	5.650	4.100
f_{θ_0}	887.7	764.3	638.6
Z_{v_i}	−0.168	−0.233	0.449
Z_{β_0}	−177.8	−205.3	−109.4
$Z_{\dot{\beta}_0}$	−1.618	−0.436	2.619
Z_w	0.168	0.233	−0.449
Z_{θ_0}	44.66	44.66	−44.39

[a] Z_{θ_0} fixed at theoretical value. [b] Z_{θ_0} free.

displays much better correlation with the model identified with Z_{θ_0} constrained than it does with the other model. In fact, it could almost be argued from this result that the theoretical model does not need any improvement.

This assessment is reinforced by Fig. 5, which appears to show that the model identified with Z_{θ_0} constrained gives, at least by visual inspection, just as good a fit with the flight-derived frequency response as the model identified with Z_{θ_0} free, certainly up to 3 Hz. In this figure, the vertical acceleration to collective gain of both identified models shown in Table 6 is compared with the frequency response derived from the sweep data. (Here, the analysis is optimized to focus on frequencies higher than the 3.5 Hz used in the identification.) However, differences become visually apparent beyond 3 Hz and it can then be argued that the characterization of the Puma obtained with Z_{θ_0} free is the more appropriate one for model validation. It is clear, then, that the use of a constraint can substantially affect the derivative values, and so care must be exercised if circumstances are such that this has to be done, e.g., if an acceptable solution cannot be obtained because of insufficient state information, such as the case in the previous section that dealt with the effects of different a priori estimates. In this case here, the impact on model validation conclusions are significant. Where a fixed constraint has to be used, a potential way forward would be to identify family of models, effectively attempting to validate theory in a parametric manner.

It is interesting to note that time-domain comparison of both models' prediction of the helicopter's response to a step input is unable to resolve this potential parameter sensitivity problem. It might be thought that this would be a particularly efficacious way of deciding which of these two models is the more appropriate representation of the Puma because of the difference in their respective Z_{θ_0} derivatives. In response to a given step, one would give a positive increment in acceleration at time zero, as opposed to the other, which would give a negative increment. Under ideal circumstances, this difference could be observed in the initial vertical response to the step input, and the more appropriate model would then be apparent. In this case, however, two aspects of the problem mask this feature. First, the differences between the two models manifest themselves only at very high frequency, which means that inputs other than pure steps are unlikely to have the frequency content required. Second, pilot neuromuscular and actuation system lags do tend to result in nominal steps actually appearing as ramps. Results to illustrate this are shown in Fig. 6, which compares the vertical acceleration response to a nominal step input in collective, measured in flight, with that predicted using both identified models. The input only has the frequency content to excite both models at the lower frequencies where both models give an excellent match with the flight-derived frequency response.

Table 7 Comparison of derivatives identified by frequency response and output-error methods

Derivative	Theoretical value	Frequency response[a]	Output error[a,b]
i_{v_i}	−9.197	−9.147 (0.0472)	−7.148 (0.38)
i_{β_0}	−36.54	−40.76 (0.5602)	−39.19 (0.50)
i_w	7.311	6.703 (0.0892)	8.360 (0.31)
i_{θ_0}	589.0	599.4 (3.0945)	609.9 (0.03)
f_{v_i}	−2.294	−4.245 (0.0248)	−3.555 (0.13)
f_{β_0}	−821.9	−836.7 (1.5973)	−804.8 (0.18)
$f_{\dot{\beta}_0}$	−18.75	−24.47 (0.0855)	−22.25 (0.18)
f_w	3.317	4.635 (0.0443)	3.721 (0.57)
f_{θ_0}	517.5	682.8 (1.3974)	638.0 (0.11)
Z_{v_i}	0.755	0.547 (0.0056)	0.266 (0.06)
Z_{β_0}	−102.3	−96.46 (0.4640)	−112.9 (1.33)
$Z_{\dot{\beta}_0}$	2.868	1.393 (0.0164)	3.766 (0.16)
Z_w	−0.628	−0.474 (0.0315)	−0.627 (0.11)
Z_{θ_0}	−79.14	−48.87 (0.3510)	−47.33 (1.09)

[a]Parameter standard deviation in parentheses.
[b]Values obtained using rank-deficient information matrix (rank 9).

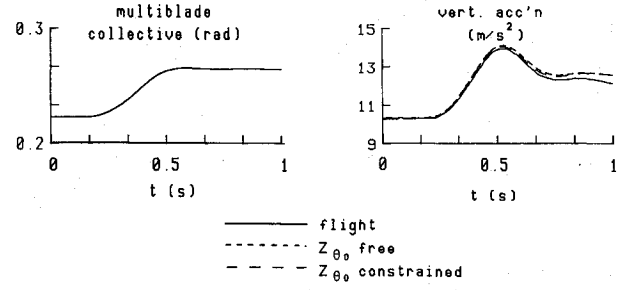

Fig. 6 Comparison of the prediction of the response to a step input given by both identified models—transfer function matching method.

The final example in this section concerns the output-error method. When a rank-deficient information matrix is used for the output-error method (indicating, on the basis of the data, implicit relationships between groups of parameters) convergence is obtained with 14 parameters, see Table 7. Theoretical flapping equation derivatives, in fact, compare more favorably with this output-error set of estimates than with any other set in the paper. This result indicates that the 14 derivatives are not entirely independent and that it is valid to consider relationships within the model structure. It also serves as a reminder that engineering judgment (in this case, the incorporation of relationships into the model) is a key component in system identification. Results obtained using rank-deficient output-error solutions are fully discussed in Ref. 14.

Discussion

This paper has sought to illustrate, by example, some aspects of model identification that can give rise to concerns over whether the identified parameters can be used with any confidence for model validation. It is the case, however, that the key to successful identification in this context lies in the expertise of the user, not only with a physical understanding of the nature of the model to be validated as well as the experimental data used. Engineering judgment plays perhaps the major part in successful system identification.

The results suggest that models incorporating higher order dynamics do not present any special difficulties in relation to identifiability if state information is available and its frequency content covers a range appropriate to the bandwidth of the dynamics of concern. The latter will have an impact on flight experiment design. For example, it could preclude the use of aircraft that cannot be excited by high-frequency control inputs because of air worthiness considerations. The actuation system characteristics may be such that they attenuate important higher frequency content in the pilot's input. The aircraft itself may have natural dynamics that are outside the frequency range across which a pilot can apply inputs. This is almost the case for the model structure examined in this paper, where the coning mode natural frequency is approximately 3 Hz. In the case of the Puma, this means conducting flight tests and identification above 3 Hz. With a Lynx or Gazelle, however, this figure would rise to 5 Hz. It is intended to investigate such topics in the future with a Lynx helicopter.

Although the paper's main concern has been the sensitivity of stability and control derivatives to the identification approach used, a model validation result inherent to the analysis of sensitivity, and further to that published previously,[4] is of complementary interest. This concerns the inflow modeling implied by the use of the lift deficiency factor given by Eq. (10). Although the flight results do confirm that the lift deficiency effects ought to be included in the theoretical model, the outstanding discrepancies between theory and flight in the coning and Z-force equations indicate that the value for C_l' of 0.55 underestimates that implied by the flight results. A value of $C_l' = 0.65$ would resolve the remaining discrepancy between theory and flight. It could be the case that the analytical basis on which the lift deficiency factor (and, therefore, the inflow model itself) is developed, is inconsistent with the real wake structure. At the relatively low thrust coefficients at which the Puma was flown for the experiments described in this paper, strong tip vortex and tail rotor interaction effects are present.[4] These effects can be minimized if the rotor is operated at high thrust coefficient,[22] and future work should re-examine the validation of a coupled 3 DOF model and the lift deficiency factor given by Eq. (10), in such a regime.

Conclusions

The general conclusion is that linearized state-space derivative models of helicopter behavior that incorporate higher order dynamics can be identified from flight test data with sufficient confidence to allow the results to be used in model validation. Although the identified coupled 3 DOF heave/coning/inflow model does not exhibit complete insensitivity to the choice of approach available for this paper, the use of engineering judgment and an awareness of the theoretical basis of the model to be validated can minimize to an acceptable extent the specific identifiability concerns highlighted here. The following specific conclusions can also be made and can relate to each item addressed in this paper.

1) The output-error and transfer function identification and fitting approaches can be used to complement one another. They gave comparable results and either can therefore be used with confidence.

2) The identified model parameters were sensitive to frequency range. This sensitivity tended to diminish above frequencies of 2.5 Hz for the inflow and flapping derivatives and 3 Hz for the Z force terms.

3) The identified model parameters in the dynamic inflow equation were sensitive to variability in the corresponding a priori estimates used as initial guesses in the parameter estimation. This can affect the assessment of which value of air mass to use with the theoretical model, although it should be noted that each identified set was self-consistent.

4) Constraining variables to reflect the similarity among derivatives in one of the theoretical models has little effect on the values of the identified derivatives. However, constraining a variable at a theoretical value can have a substantial impact that could influence model validation. Full and rank-deficient output-error solutions do indicate that the 14 derivatives are not wholly independent and that some form of relational constraint in the model structure, or constraint derived from the properties of the test data, would be appropriate.

5) With the transfer function matching approach, identified derivatives exhibited substantial sensitivity to test run. This was attributed to the use of identified frequency re-

sponses with poor coherence. Use of responses with good coherence gave identified derivatives that were vastly less sensitive to test runs. A frequency response with good coherence has been defined as that for which $<5\%$ of the frequency points have coherence <0.8.

References

[1]Padfield, G. D., "Theoretical Modelling for Helicopter Flight Dynamics; Development and Validation," *Proceedings of the 16th Congress of the International Council of the Aeronautical Science,* AIAA, Washington, DC, 1988.

[2]Houston, S. S., "Identification of Factors Influencing Rotorcraft Heave Axis Damping and Control Sensitivity," Royal Aerospace Establishment, Bedford, England, UK, TR-88067, Jan. 1989.

[3]Houston, S. S., "Identification of a Coupled Body/Coning/Inflow Model of Puma Vertical Response in the Hover," *Vertica,* Vol. 13, No. 3, 1989, pp. 229–249.

[4]Houston, S. S., and Tarttelin, P. C., "Theoretical and Experimental Correlation of Helicopter Aeromechanics in Hover," *Proceedings of the 45th Annual Forum of the American Helicopter Society,* Boston, MA, May 1989.

[5]Feik, R. E., and Perrin, R. H., "Identification of an Adequate Model for Collective Response Dynamics of a Sea King Helicopter in Hover," *Vertica,* Vol. 13, No. 3, 1989, pp. 251–265.

[6]Blackwell, J., Feik, R. A., and Perrin, R. H., "Identification of Rotor Dynamic Effects in Flight Data," *Proceedings of the 15th European Rotorcraft Forum,* Amsterdam, The Netherlands, Sept. 1989.

[7]Black, C. G. et al., "System Identification Strategies for Helicopter Rotor Models Incorporating Induced Flow," *Proceedings of the 14th European Rotorcraft Forum,* Milan, Italy, Sept. 1989.

[8]Bradley, R., Black, C. G., and Murray-Smith, D. J., "Glauert Augmentation of Rotor Inflow Dynamics," *Proceedings of the 15th European Rotorcraft Forum,* Amsterdam, The Netherlands, Sept. 1989.

[9]Du Val, R. et al., "Identification of a Coupled Flapping/Inflow Model for the Puma Helicopter from Flight Test Data," *Vertica,* Vol. 13, No. 3, 1989, pp. 267–274.

[10]Padfield, G. D., "A Theoretical Model of Helicopter Flight Mechanics for Application to Piloted Simulation," Royal Aerospace Establishment, Bedford, England, UK, TR-81048, April 1981.

[11]Chen, R. T. H., and Hindson, W. S., "Influence of Dynamic Inflow on the Helicopter Vertical Response," *Vertica,* Vol. 11, Nos. 1, 2, 1987, pp. 77–91.

[12]Johnson, W., *Helicopter Theory,* Princeton University Press, Princeton, NJ, 1980, Chaps. 10 and 11.

[13]Black, C. G., Murray-Smith, D. J., and Padfield, G. D., "Experience with Frequency-Domain Methods in Helicopter System Identification," *Proceedings of the 12th European Rotorcraft Forum,* Garmisch-Partenkirchen, Germany, Sept. 1986.

[14]Black, C. G., "A Frequency-Domain Output-Error Identification of a State-Space Model for Heave Dynamics (Incorporating Induced Flow) Using a Limited Measurement Set," Dept. of Aerospace Engineering, University of Glasgow, Rept. 9002, July 1989.

[15]Bendat, J. S., and Piersol, A. G., *Engineering Applications of Correlation and Spectral Analysis,* Wiley, New York, 1980.

[16]Priestly, M. B., *Spectral Analysis and Tirne Series,* Academic, New York, 1981.

[17]Houston, S. S., and Horton, R. I., "The Identification of Reduced-Order Models of Helicopter Behavior for Handling Qualities Studies," *Proceedings of the 13th European Rotorcraft Forum,* Arles, France, Sept. 1987.

[18]Black, C. G., "Consideration of Trends in Stability and Control Derivatives from Helicopter System Identification," *Proceedings of the 13th European Rotorcraft Forum,* Arles, France, Sept. 1987.

[19]Maine, R. E., and Iliff, K. W., "Use of Cramer-Rao Bounds on Flight Data with Colored Residuals," *Journal of Guidance, Control, and Dynamics,* Vol. 4, No. 2, 1981, pp. 207–213.

[20]Carpenter, P. J., and Fridovitch, B., "Effect of a Lipid Blade-Pitch Increase on the Thrust and Induced-Velocity Response of a Full-Scale Helicopter Rotor," NACA TN-3044, Nov. 1953.

[21]Pitt, D. M, and Peters, D. A., "Theoretical Prediction of Dynamic-Inflow Derivatives," *Vertica,* Vol. 5, No. 1, 1981, pp. 21–34.

[22]Lorber, P. F., Stauter, R. C., and Landgrebe, A. J., "A Comprehensive Hover Test of the Airloads and Airflow of an Extensively Instrumented Model Helicopter Rotor," *Proceedings of the 45th Annual Forum of the American Helicopter Society,* Boston, MA, May 1989.